Supplement of Atmos. Chem. Phys., 17, 6565–6581, 2017
https://doi.org/10.5194/acp-17-6565-2017-supplement

Supplement of

Regional background O_3 and NO_x in the Houston–Galveston–Brazoria (TX) region: a decadal-scale perspective

Loredana G. Suciu et al.

Correspondence to: Loredana G. Suciu (lgs4@rice.edu)

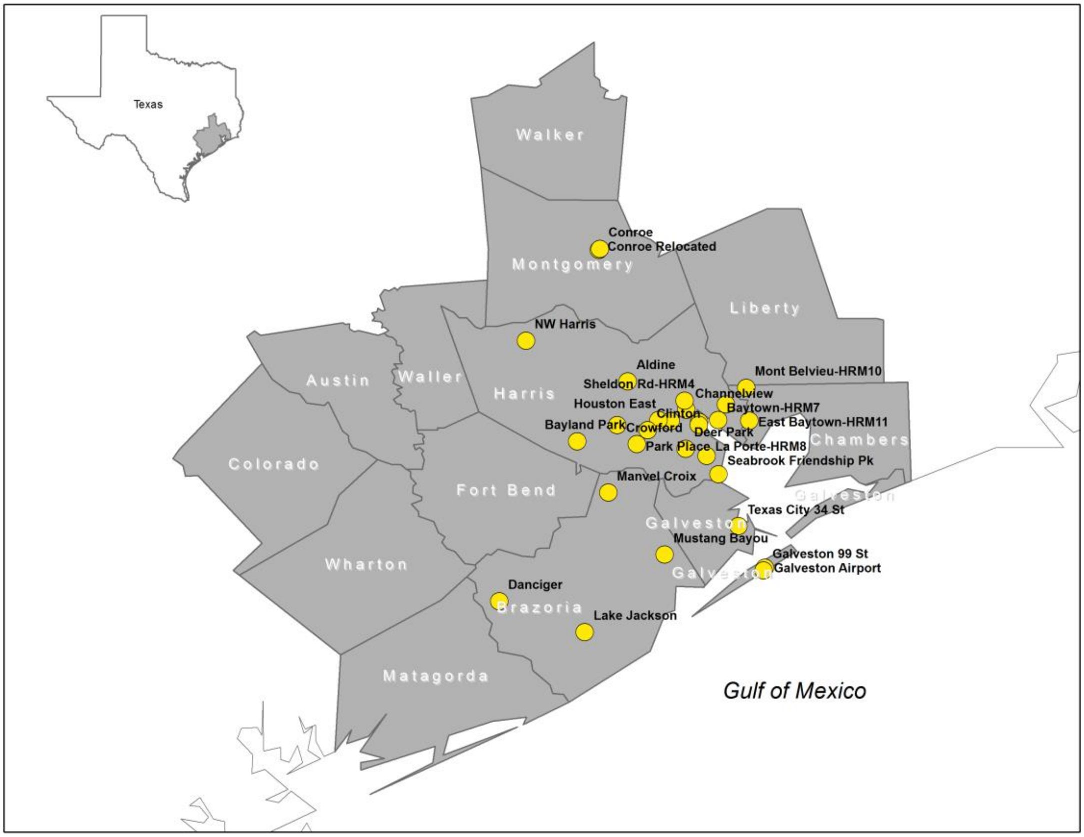

Figure S1: The Houston-Galveston-Brazoria (HGB) region (grey) and the TCEQ monitoring sites (yellow dots) used in this work.

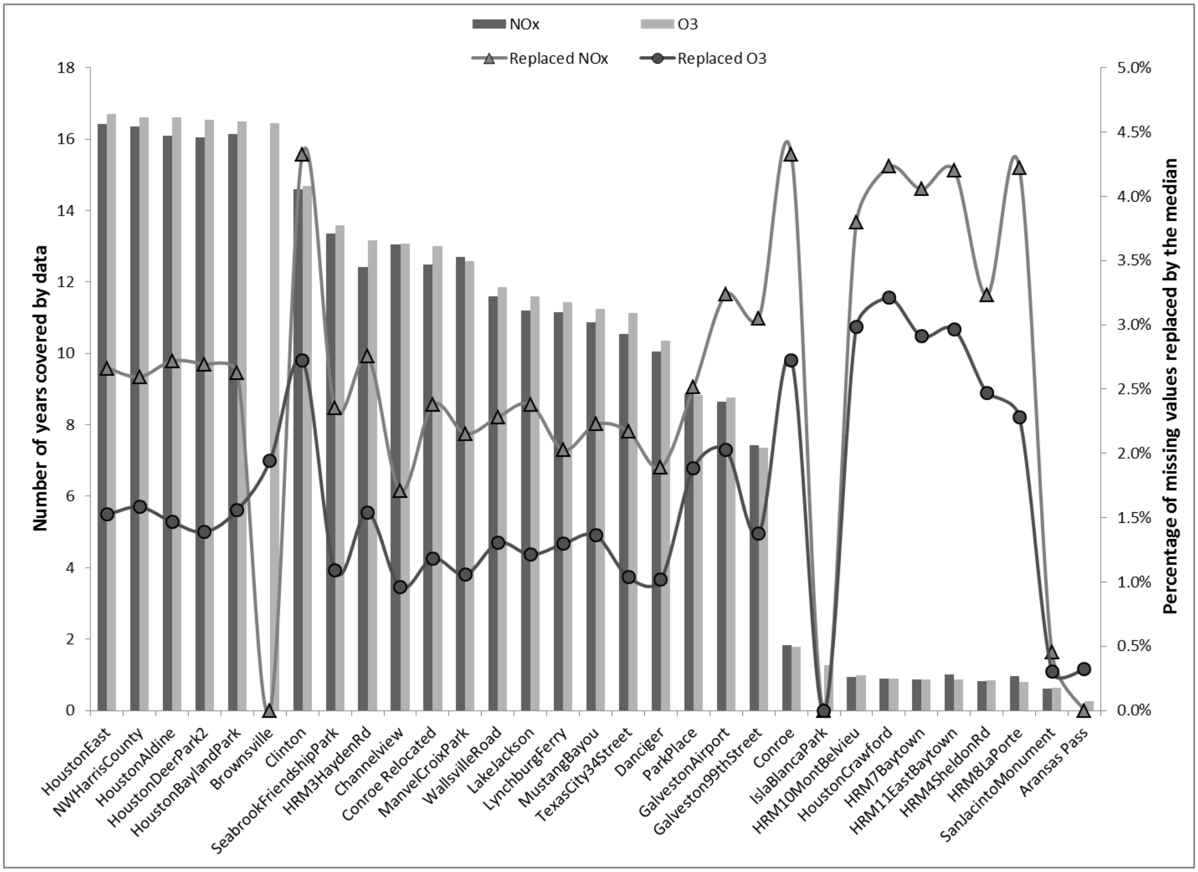

Figure S2: Statistics of data availability and replacement by the hourly median for the sites used in this work.

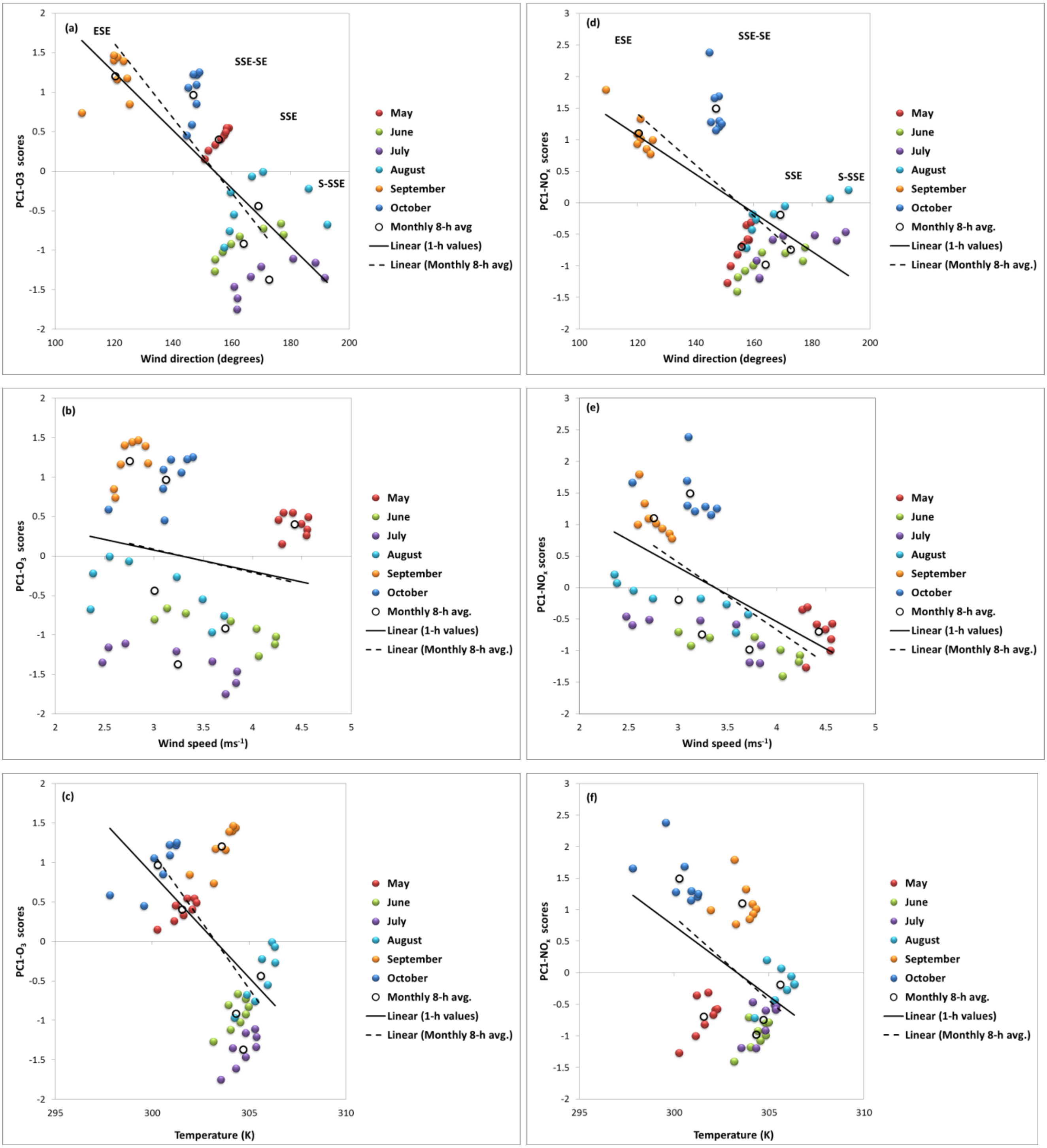

Figure S3: Relationships between meteorological variables and the first component for O_3 (a-c) and NO_x (d-f). Dots represent daytime hours (10 am - 6 pm) in each month. Empty circles are the monthly 8-h averages.

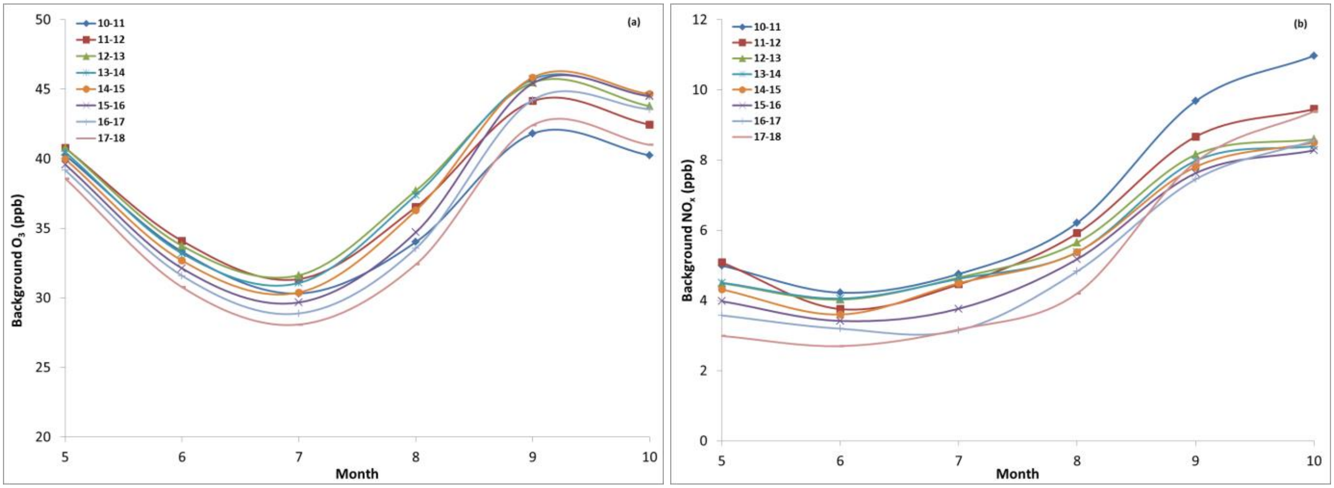

Figure S4: The 6-month trends in background O_3 (a) and background NO_x (b) for each daytime hour.

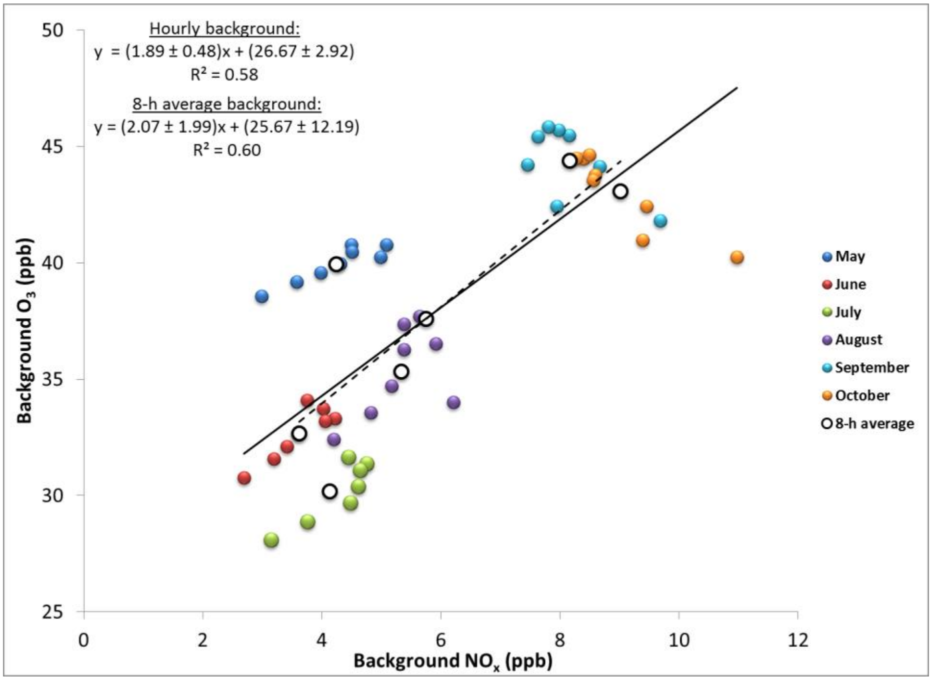

Figure S5: Relationship between PCA-estimated background O_3 and NO_x at both 1-h and 8-h levels. Dots represent daytime hours (10 am - 6 pm) in each month. Empty circles are the monthly 8-h averages.

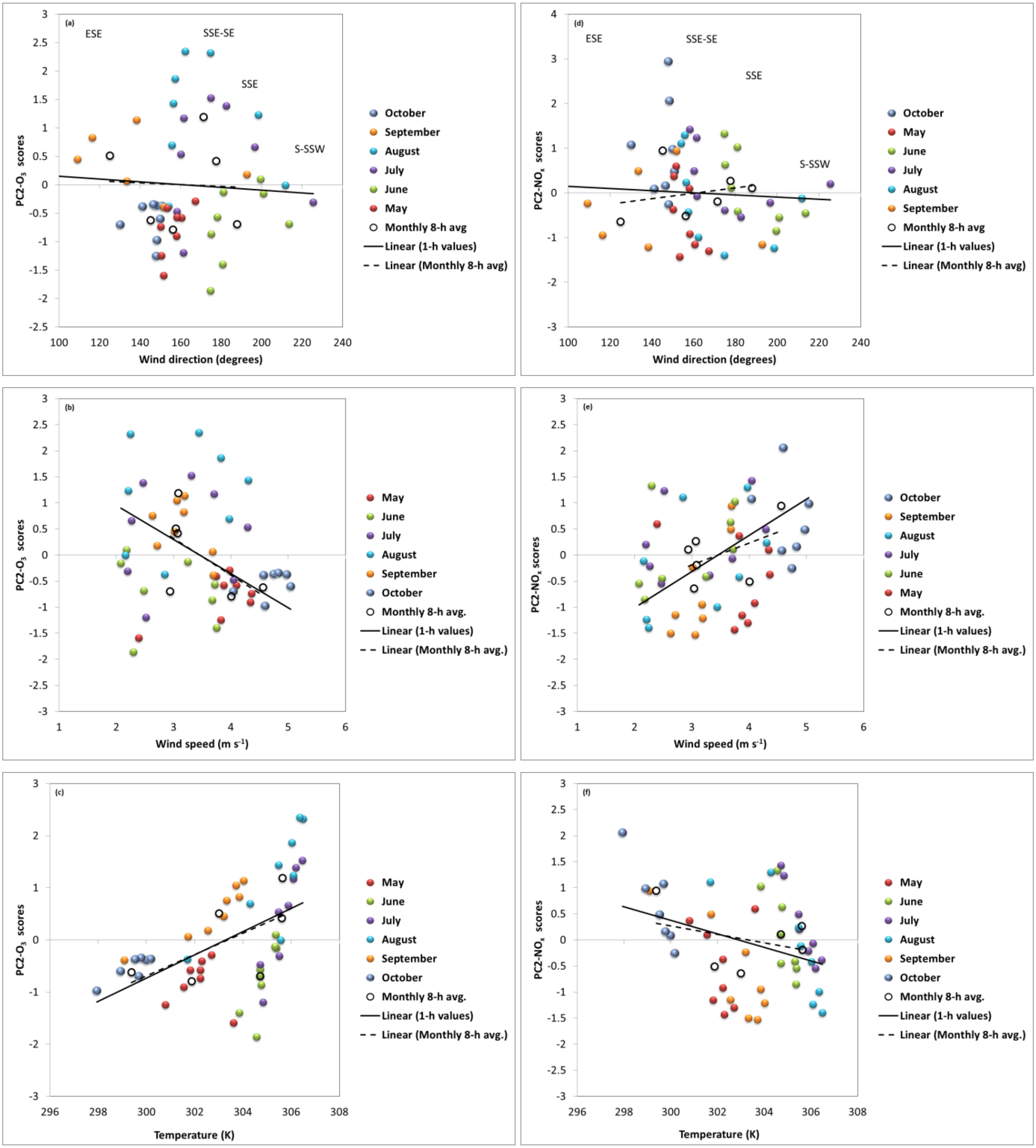

Figure S6: Relationships between meteorological variables and the second component for O_3 (a-c) and NO_x (d-f). Dots represent daytime hours (10 am - 6 pm) in each month. Empty circles are the monthly 8-h averages.

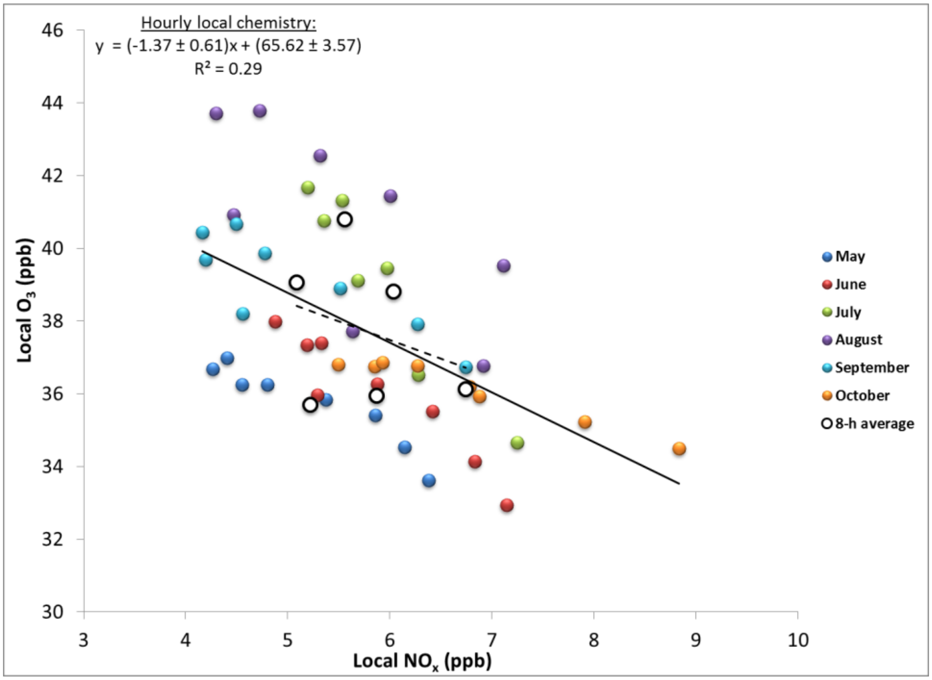

Figure S7: Relationship between PCA-estimated local O_3 and NO_x at the 1-h level. Dots represent daytime hours (10 am - 6 pm) in each month. Empty circles are the monthly 8-h averages.

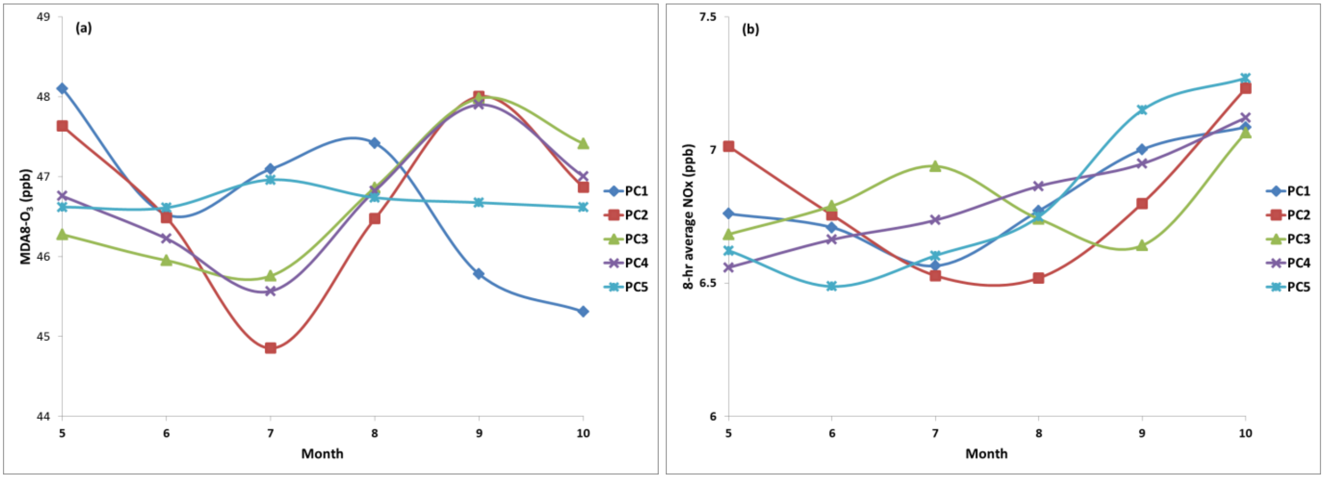

Figure S8: The 6-month trends of principal components converted to MDA8-O_3 (a) and 8-h average NO_x (b) to help distinguish between regional and local contributions. Points represent the 17-year average values. The regional contributions are expected to peak in spring and late summer/early fall, and drop in mid-summer. The opposite is expected from local contributions.

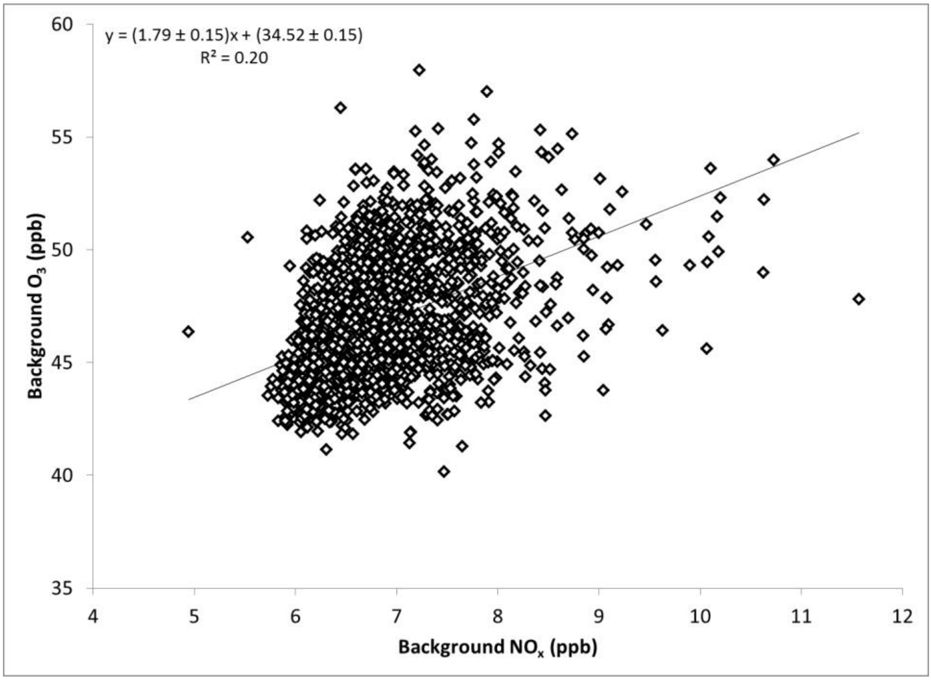

Figure S9: Relationship between regional background O_3 and NO_x (Approach A).

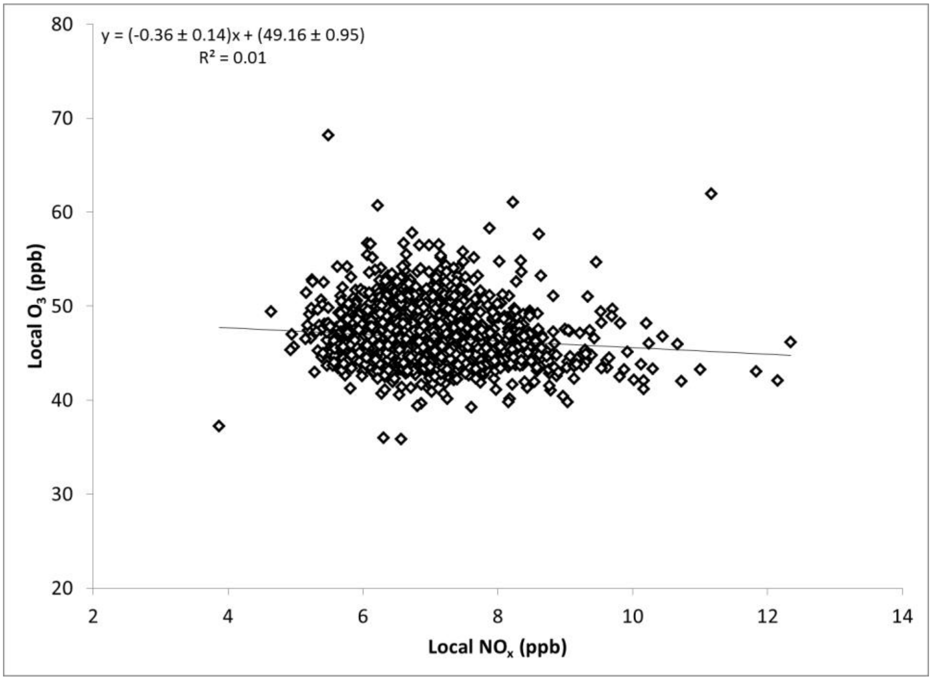

Figure S10: Relationship between local O_3 and NO_x (Approach A).

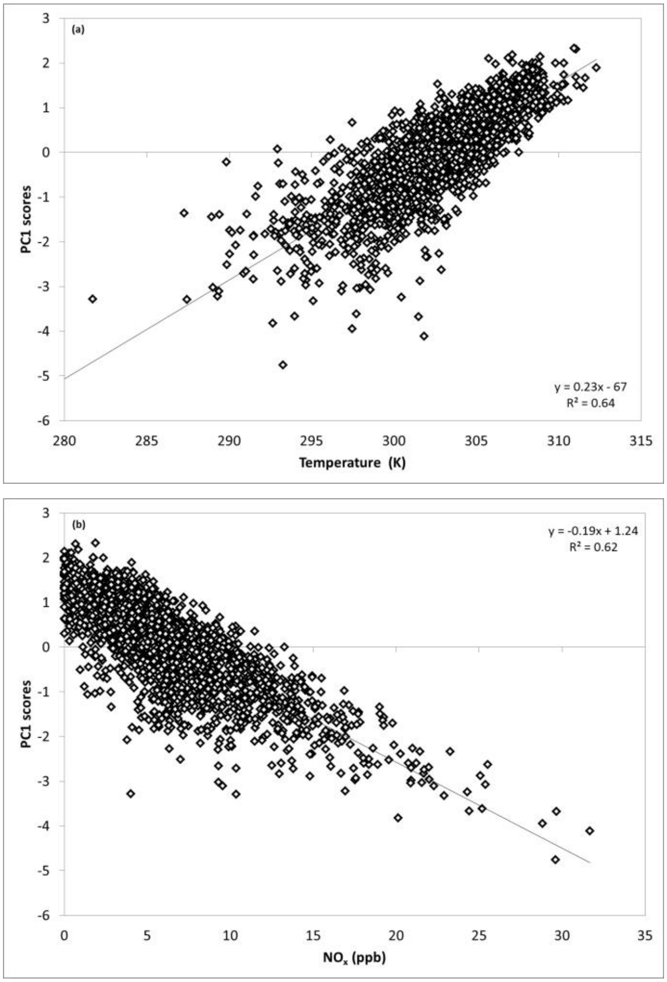

Figure S11: Example of a "NO_x-T" site (Aldine) where temperature (a) and NO_x (b) explain the variation in PC1 scores.

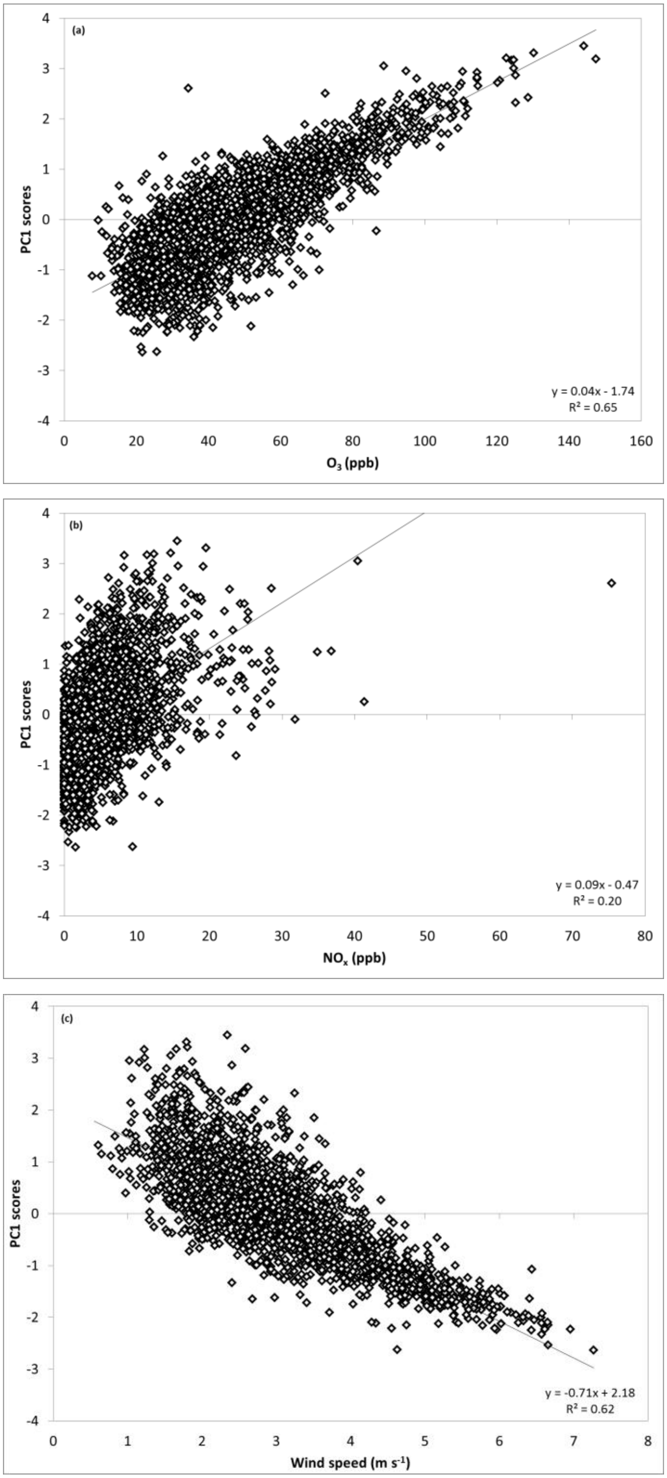

Figure S12: Example of an "O_3-NO_x-WS" site (Bayland Park) where O_3 (a), NO_x (b) and WS (c) explain the variation in PC1 scores.

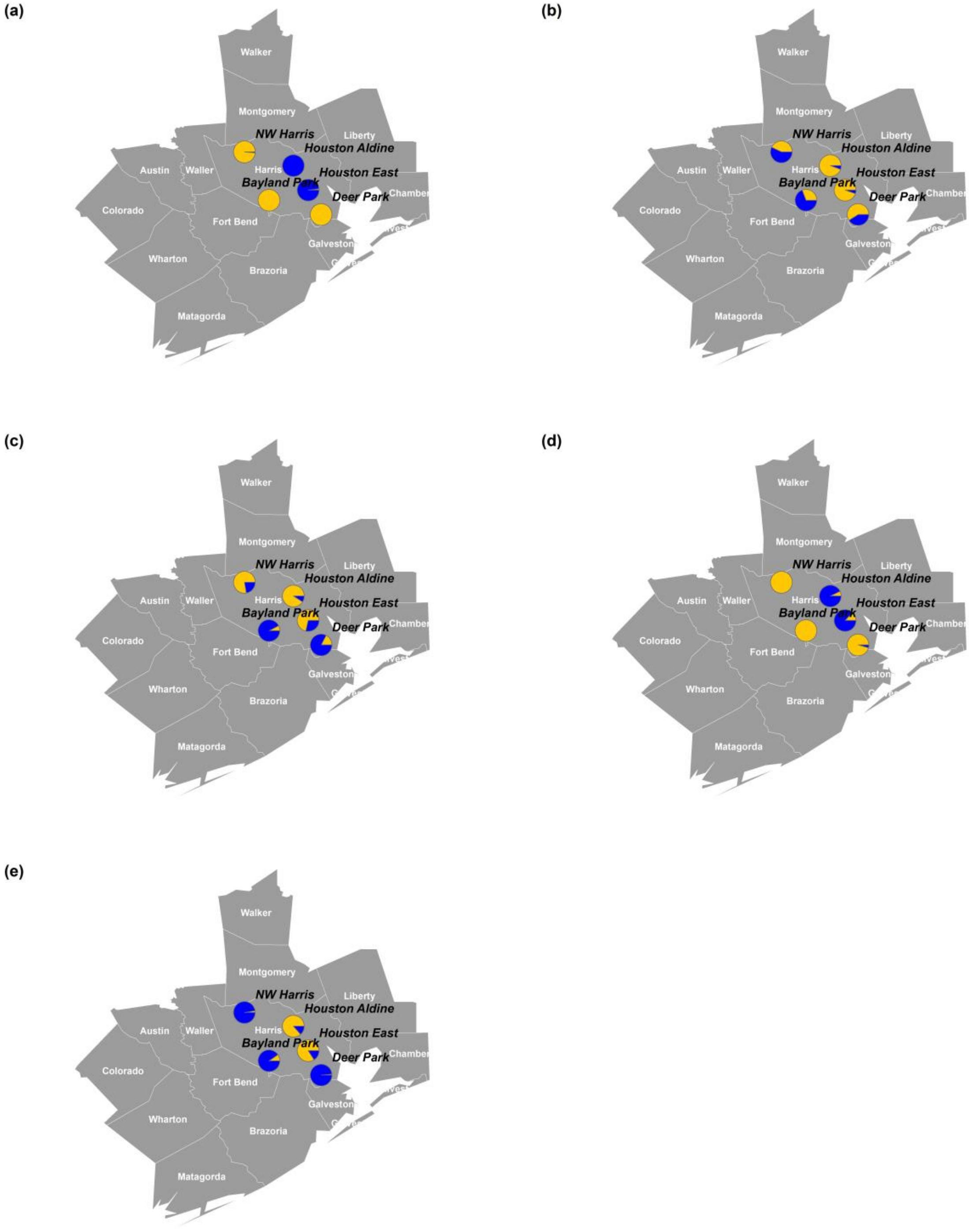

Figure S13: Partition of O_3 (a), NO_x (b), WD (c), WS (d) and T (e) between the two components (PC1 in yellow and PC2 in blue).

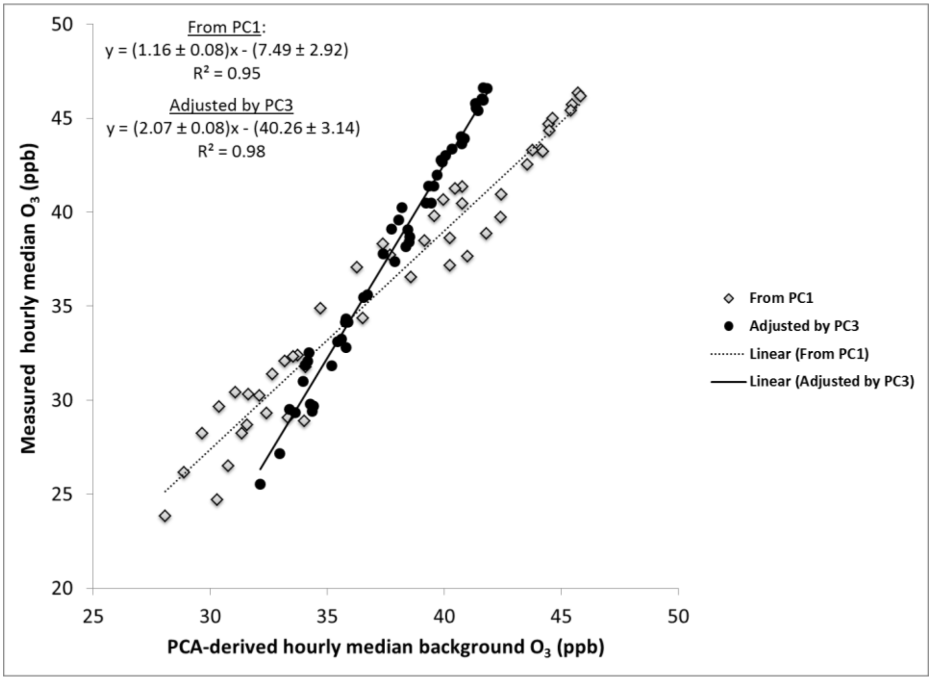

Figure S14: Measured hourly median O_3 (average of 16-19 sites) vs. estimated background O_3 from PCA.

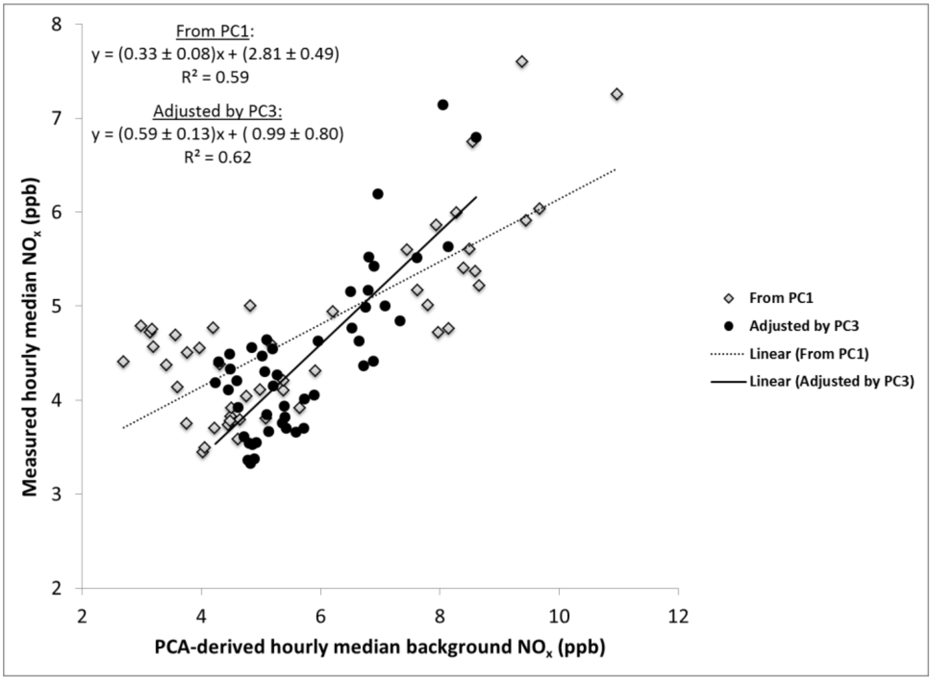

Figure S15: Measured hourly median NO_x (average of 15-18 sites) vs. estimated background NO_x from PCA.

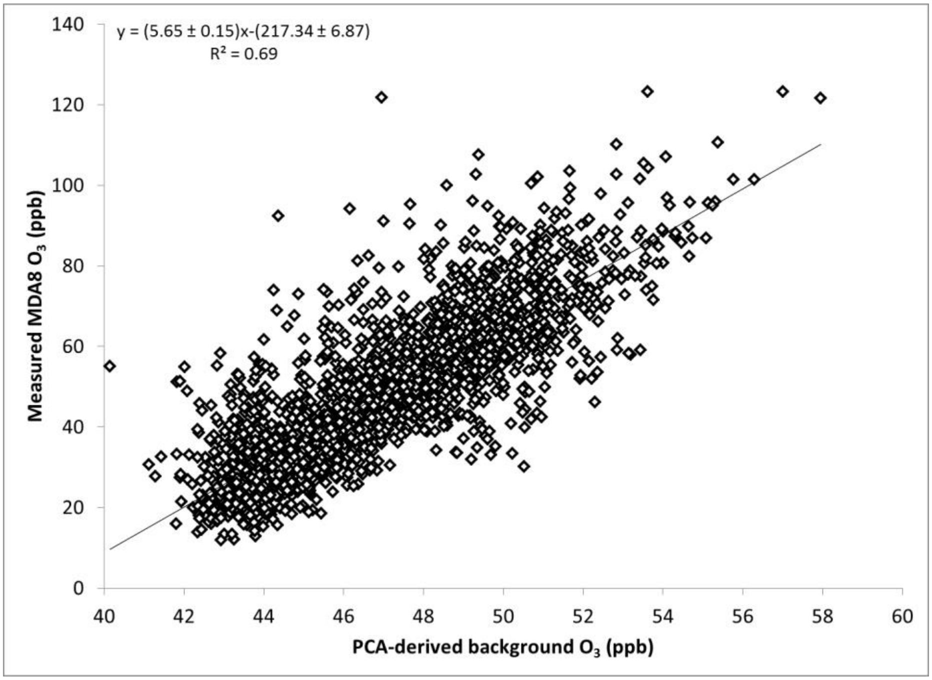

Figure S16: Measured MDA8-O_3 (average of 5 sites) vs. background O_3 derived from PCA (Approach A).

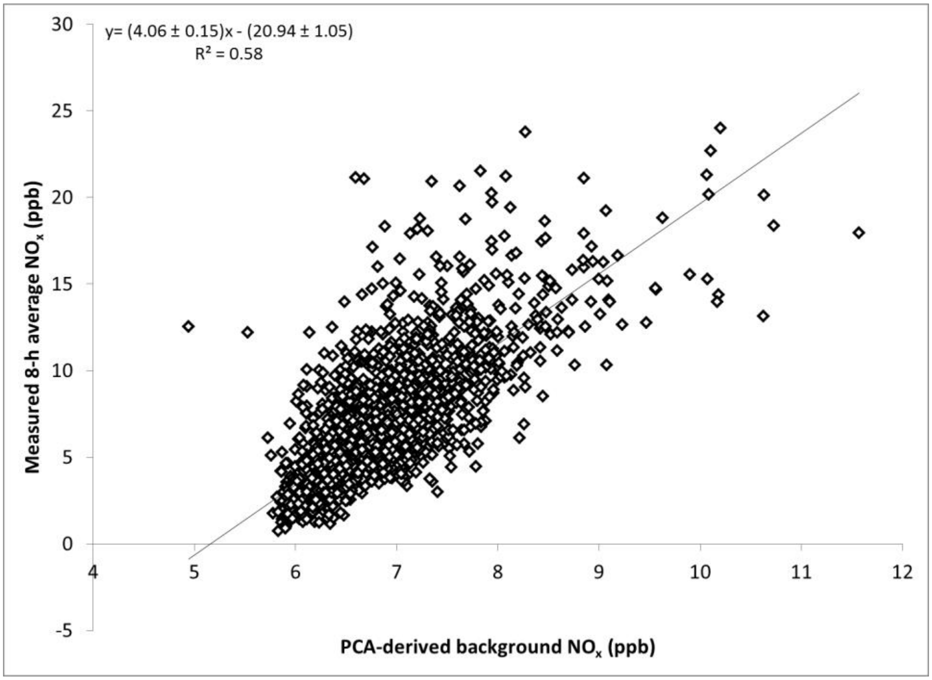

Figure S17: Measured 8-h average NO_x (average of 5 sites) vs. background NO_x from PCA (Approach A).

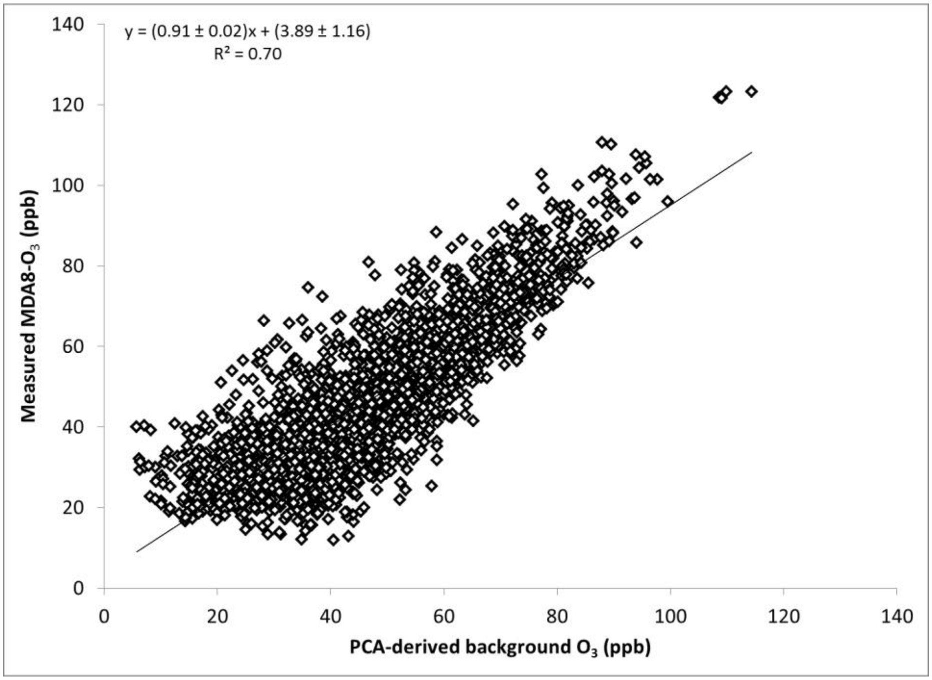

Figure S18: Measured MDA8-O_3 (average of 5 sites) vs. background O_3 derived from PCA (Approach B).

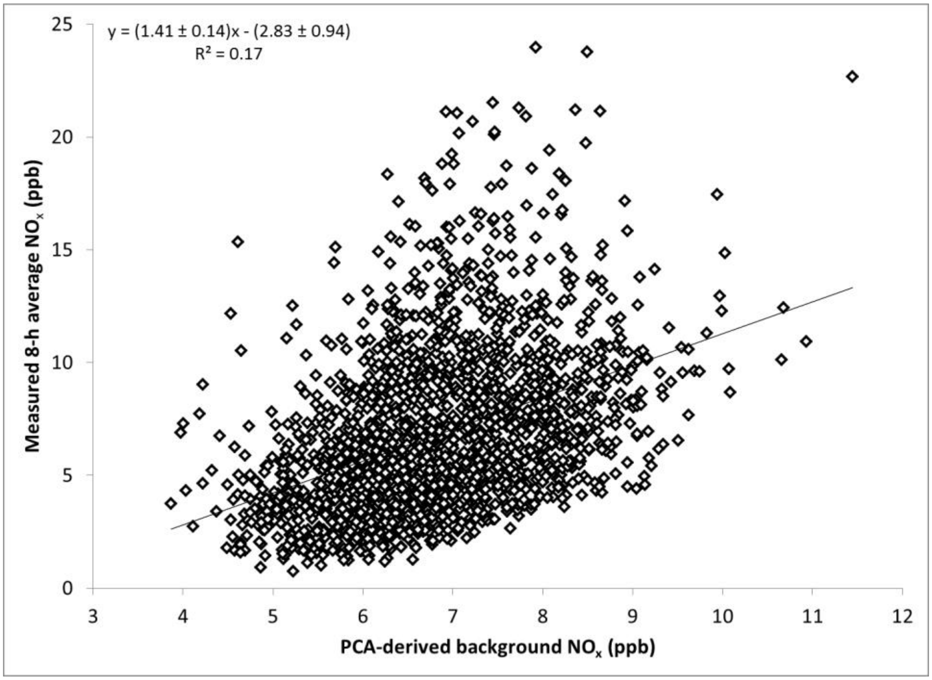

Figure S19: Measured 8-h average NO_x (average of 5 sites) vs. background NO_x from PCA (Approach B).

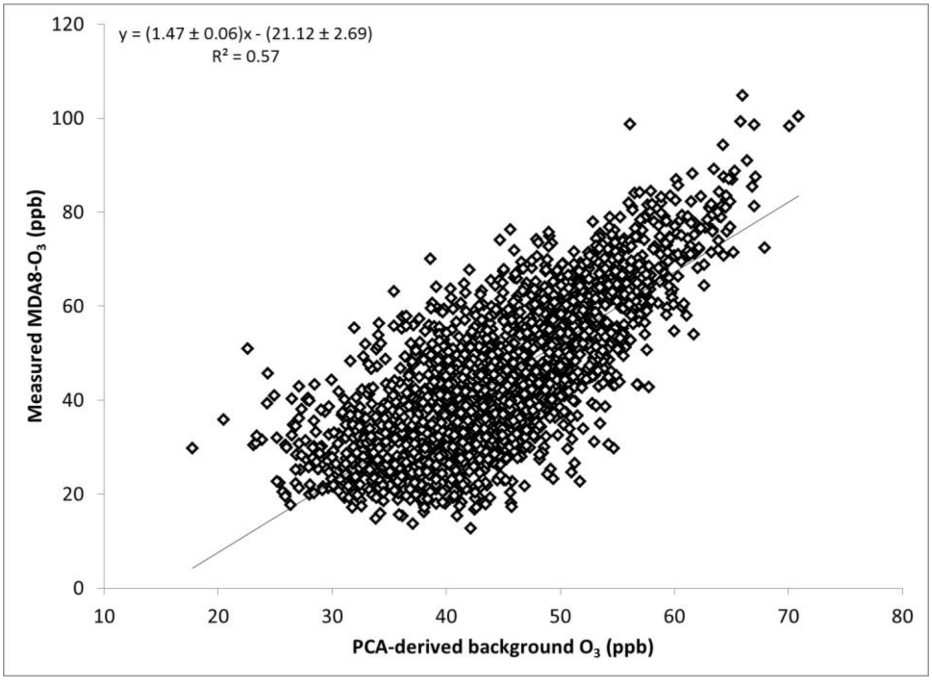

Figure S20: Measured MDA8-O_3 (average of 10 sites) vs. background O_3 derived from PCA (Approach C).

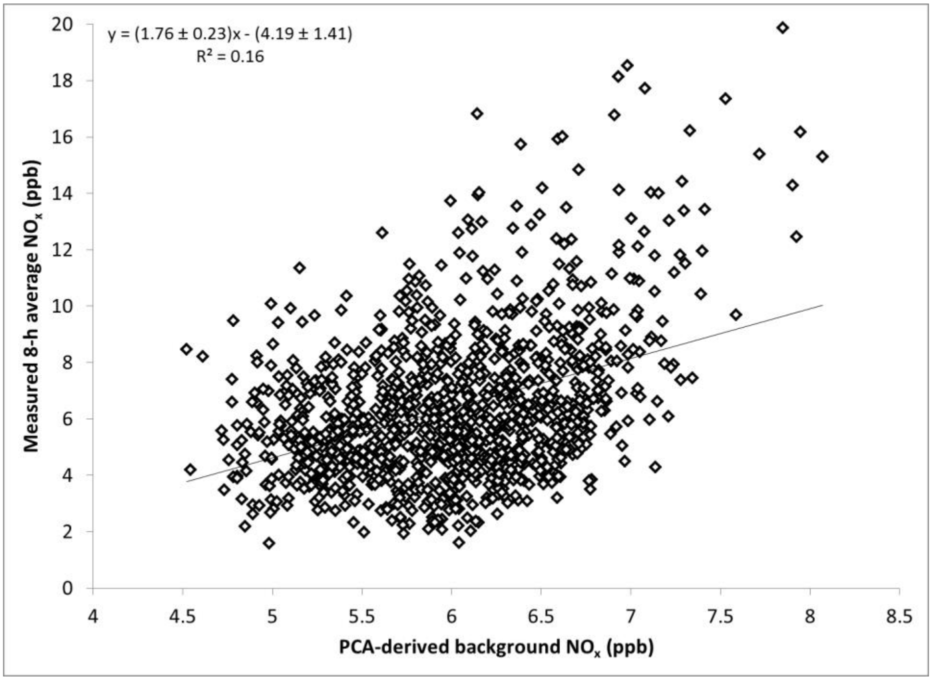

Figure S21: Measured 8-h average NO_x (average of 10 sites) vs. background NO_x from PCA (Approach C).

Background NO_x

1. Considerations for potential biases in background NO_x

Background NO_x estimates in this study may be subject to two biases: the time-averaging scale and the overdetection of NO_x by the measuring instrument. Both biases lead to overestimation of background NO_x. Thus, our estimate provided an upper bound of background NO_x. In the following sections we discuss, estimate and use these biases to quantify the long-term averages and temporal trends in lower bound background NO_x. Because we subtract these biases from the previously determined background NO_x (*aka* upper bound), our new estimate of background NO_x is a lower bound.

1.1 Bias due to time-averaging

The 8-h averaging of NO_x may not adequately capture background NO_x. This could occur because the temporal variability in NO_x and O_3 are different. For our PCA approach in which we co-varied chemistry and meteorology, it was necessary that the averaging of NO_x, WS, WD and T occur over the same time period as for MDA8 O_3 to match the analysis time scale for all the variables at which their covariance would be meaningful. For instance, O_3 and T vary over larger temporal scales compared to NO_x and WS. However, because O_3 and NO_x have different temporal dynamics, this may introduce bias. In our study, we selected the maximum 8-h average O_3 value which, therefore, drove our selection of the corresponding 8-h average NO_x, WD, WS and T values, potentially biasing high our background NO_x estimate and its temporal trends.

To determine how much we may have overestimated background NO_x due to time-averaging, we have compared the season-scale 8-h and 1-h background NO_x values (Fig. 5). We found that due to differing temporal dynamics of O_3 and NO_x the analytical focus on the time of MDA8 O_3 occurrence may lead to an overestimation of the 8-h background NO_x of approximately 18%."

1.2 Bias due to overdetection of NO_x by the measuring instrument

The combined chemiluminescence/molybdenum conversion method used to measure NO_x also detects other reactive nitrogen (NO_y) species (PAN, HNO_3, organic nitrates/nitrites, etc.) as NO_x (Winer et al., 1974). Because NO_2 is determined by difference from total NO_x (after its conversion to NO) and NO (measured by chemiluminescene prior to the conversion of other NO_y species to NO), NO_2 is actually not measured by this method, preventing us from using it in the analysis of background NO_x or using the O_x metric.

Although there is a variation in the instrument conversion efficiency for individual species, we assume 100% conversion for all species to generate an upper-bound estimate of error, allowing us to use published field studies to determine the potential error in overdetecting NO_x. A two-month field study (Luke et al., 2010) individually measured NO_x species (NO, NO_2) and NO_z species (HNO_3, PAN, HONO and p-NO_3^-) during daytime at the top of the Moody Tower (University of Houston). The dominant NO_z species, representing fractions of NO_y during the most photochemically active window (11 am - 5 pm), were HNO_3 (17-19.5 %) and PAN (12-14.8%), while other species (HONO and p-NO_3^-) showed minor contributions (<1-1.5%).

Based on the total NO_z fraction and assuming that NO_z would be detected as NO_x in the TCEQ instruments, we inferred that the overdetection of NO_x by the chemiluminescense/molybdenum conversion method was at most approximatively 30%. This estimate is likely to be high for two reasons. First, as described above, instrument conversion of PAN, HNO_3 and higher nitrogen oxides is not likely to be 100%. Second, the extrapolation of this error estimate to the season-scale (May-Oct.) includes periods of time when photochemistry is not as active as the summer, leading to less production of NO_z species.

1.3 Corrections of background NO_x for overall bias

Based on these two potential errors and using error propagation, we estimated a maximum overall bias of 35%. By applying this overall bias to the upper bound of background NO_x (the one uncorrected for biases), we obtained a lower estimate of the background, which we refer to as the lower bound of 8-h background NO_x (see Table 5). Using the bias due to the measurement method only, we estimated the lower bound of 1-h background NO_x (Table 5). Given that the bias due to overdetection of NO_x was based on late summer only, a period highly representative of significant photochemistry, we hypothesize that the actual season-scale (May-Oct.) ground-level background NO_x falls in between these two bounds. The lower bound of background NO_x is shifted to lower ranges compared to the uncorrected values by approximately 2 ppb. Likewise, the regression coefficients (slope and intercept) decreased proportional to the overall bias (by ca. 35%). Figure S22 shows the lower bound of 8-h background NO_x trends for all approaches (A-C). The long-term averages and trend parameters for these estimates are summarized in Table 5.

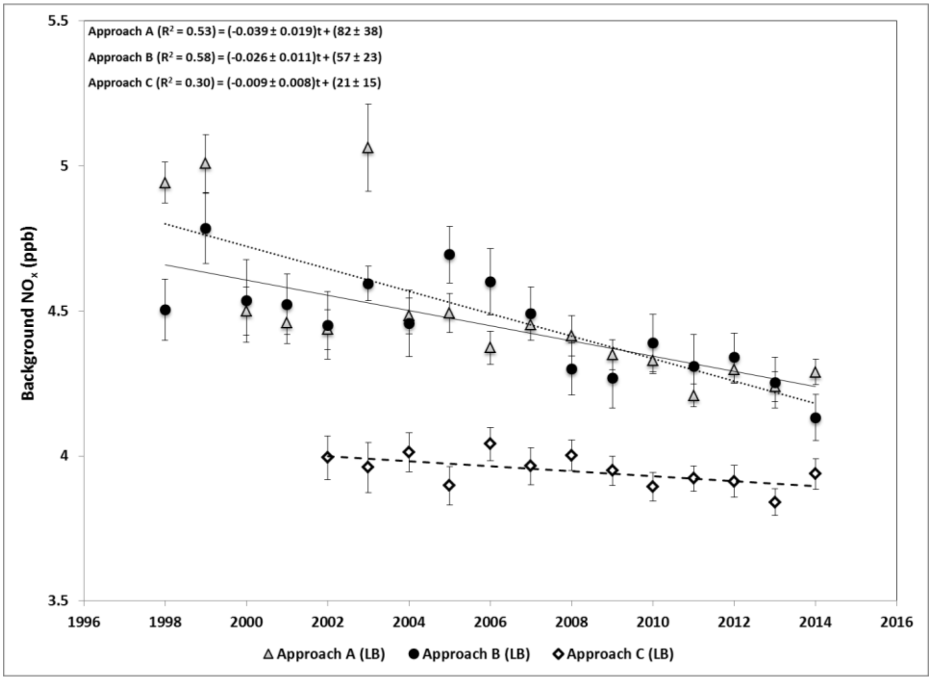

Figure S22: Temporal trends in lower bound of background NO_x

References

Luke, W. T., Kelly, P., Lefer, B.L., Flynn, J., Rappenglück, B., Leuchner, M., Dibb, J., E., Ziemba, L. D., Anderson, C. H., Buhr, M.: Measurements of primary trace gases and NOy composition in Houston, Texas, Atmos. Environ., 44, 4068-4080, doi:10.1016/j.atmosenv.2009.08.014, 2010.

Winer, A. M., Peters, J. W., Smith, J. P., Pitts, J. N. Jr.: Response of commercial chemiluminescent NO-NO_2 analyzers to other nitrogen-containing compounds, Environ. Sci. Technol., 8(13), 1118-1121, doi: 10.1021/es60098a004, 1974.